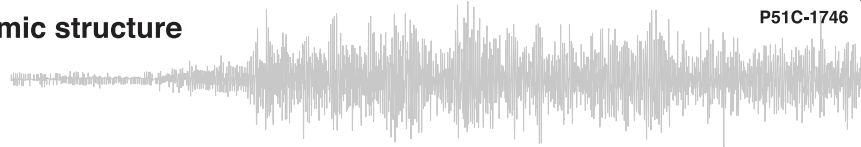


GRAIL refinements to lunar seismic structure

Renee C. Weber¹, Nicholas C. Schmerr²

- 1. NASA Marshall Space Flight Center
- 2. University of Maryland



Introduction and background

Joint interpretation of disparate geophysical datasets helps reduce drawbacks that can result from analyzing them individually. The Apollo seismic network was situated on the lunar nearside surface in a roughly equilateral triangle having sides approximately 1000 km long, with stations 12/14 nearly co-located at one corner (Figure 1). Due to this limited geographical extent, near-surface ray coverage from moonquakes is low, but increases with depth (Figure 2). In comparison, gravity surveys and their resulting gravity anomaly maps have traditionally offered optimal resolution at crustal depths. Gravimetric maps and seismic data sets are therefore well suited to joint inversion, since the complementary information reduces inherent model ambiguity.

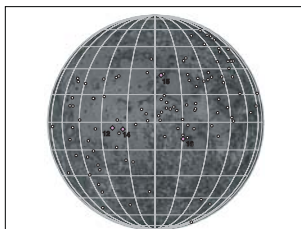


Figure 1: Map of the lunar near side (15° grid lines) showing the locations of the Apollo seismic stations and the epicenter locations of a sampling of deep moonquakes. Stations are, from West, Apollo 12, 14, 15, and 16.

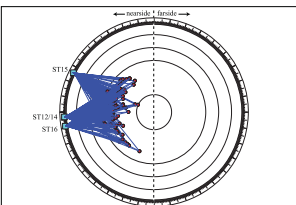


Figure 2: Cross-section showing P-wave coverage from deep moonquakes at the Apollo seismic station locations. Ray paths are projected onto the plane that slices the Moon along the prime meridian. Lateral sampling of rays is small near the surface (limited to the regions directly beneath the Apollo stations), and gradually increases with depth, with the mid-mantle most densely sampled.

Previous joint inversions of the Apollo seismic data (seismic phase arrival times) and Clementine- or Lunar Prospector-derived gravity data (mass and moment of inertia) attempted to recover the subsurface structure of the Moon by focusing on hypothetical lunar compositions that explored the density/velocity relationship. These efforts typically searched for the best fitting thermodynamically calculated velocity/density model, and allowed variables like core size, velocity, and/or composition to vary freely.

Seismic velocity profiles previously derived from the Apollo seismic data through inversion of travel times vary both in the depth of the crust and mantle layers, and the seismic velocities and densities assigned to those layers. The lunar mass and moment of inertia likewise only constrain gross variations in the density profile beyond that of a uniform density sphere. As a result, composition and structure models previously obtained by jointly inverting these data retain the original uncertainties inherent in the input data sets.

We will perform a joint inversion [1] of Apollo seismic delay times and gravity data collected by the GRAIL lunar gravity mission, in order to recover seismic velocity and density as a function of latitude, longitude, and depth within the Moon. We will relate density (ρ) to seismic velocity (v) using a linear relationship that is allowed to be depth-dependent [2]. The corresponding coefficient (B) can reflect a variety of material properties that vary with depth, including temperature and composition. The inversion seeks to recover the set of ρ , v , and B perturbations that minimize (in a least-squares sense) the difference between the observed and calculated data.

Joint seismic and gravity inversion

	observed data	calculated data
seismic data	P- and S-wave arrival times read from recorded seismograms	P- and S-wave arrival times predicted from existing structure model
gravity data	map-projected radial gravity anomaly	a space-dependent scalar estimated point-by-point from the input layer-cake velocity and density model

The model is parameterized using density blocks and velocity nodes (nodes are placed in the middle of each density block). The B-coefficient links density and velocity in each horizontal layer. The lateral and depth extent of the modeled region is dictated by the seismic data coverage. Lateral ray coverage is limited to the near side (Figure 3) due to the dearth of farside sources. Vertical ray coverage from moonquakes does not extend deeper than ~1200km due to the lack of farside receivers and attenuation effects of the core. We define the base of our model at 700 km to maximize the number of rays piercing the base layer.

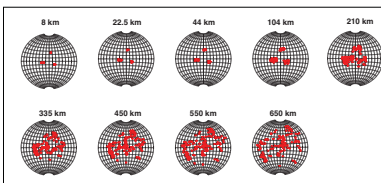


Figure 3: Pierce-points (red dots) for P-wave rays at each of the modeled layer boundaries. Shallow ray coverage is sparse, but increases with depth.

The initial seismic velocity model is taken as an average of a representative sample of published models (Figure 4).

GRAIL gravity coverage is global (Figure 5). To prevent edge effects, we model the entire extent of the nearside, leaving out those nodes that are not pierced by seismic rays.

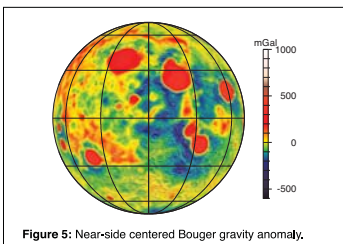


Figure 5: Near-side centered Bouguer gravity anomaly.

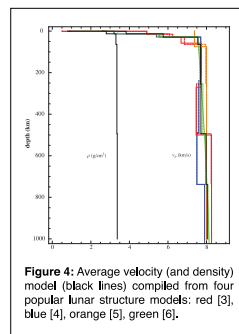


Figure 4: Average velocity (and density) model (black lines) compiled from four popular lunar structure models: red [3], blue [4], orange [5], green [6].

Initial results - coarse grid

The velocity, density, and B-coefficient perturbations obtained for every layer after each inversion are applied to the reference model, and the entire process can be repeated iteratively until the root-mean-square misfit stabilizes (Figure 6). This results in a final model that best fits the constraints jointly imposed by the seismic and gravity observations. Results for a sample run on a coarse grid are shown in Figures 7 and 8.

Figure 6: Flow chart showing iterative inversion process.

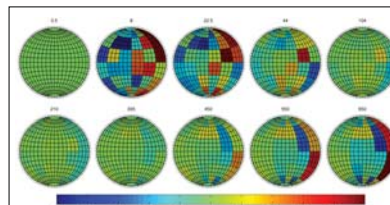
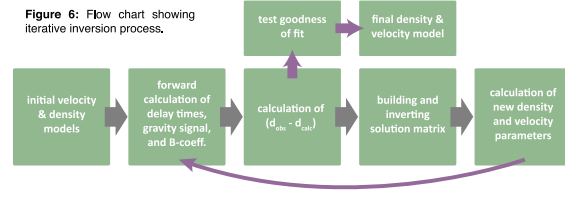


Figure 7: Near-side density anomaly (percent deviation from input model) resulting from the joint inversion, at the modeled layer boundaries. Density blocks are 30° on a side.

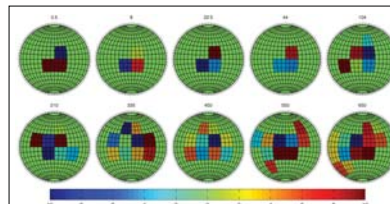


Figure 8: Corresponding near-side P-wave velocity anomaly (percent deviation from input model) resulting from the joint inversion, at the modeled layer boundaries. Velocity nodes are centered on each density block.

test inversion details

- lateral grid size: 6 x 6 @ 30°
- # of depth interfaces: 10
- # of moonquakes: 68 (located, near-side sources with visible P-wave arrivals)
- # of viable rays: 140
- # of inversion iterations: 2
- decrease of gravity RMS: 8.6%
- decrease of delay time RMS: 0.6%

current issues

The inversion is quite sensitive to the parameterization and tends to diverge rapidly if the grid size is too large. A smaller grid produces a more stable inversion, but runs the risk of producing a signal that doesn't actually exist.

The inversion is also sensitive to the initial model values. A depth-dependent relationship for the density and velocity standard deviations may prevent the inversion from attempting to concentrate large contrasts in the upper portions of the model.

References: [1] O'Donnell, J. F.; Daly, E.; Tiberti, C.; Bastow, I. D.; O'Reilly, B. M.; Fleadman, F. W.; Hauser, F. (2011) Lithosphere-asthenosphere interaction beneath Ireland from joint inversion of teleseismic P-wave delay times and GRACE gravity. *Geophys. J. Int.* 184, 1379–1396. [2] Zeyen, H.; Achauer, U. (1997) Joint inversion of teleseismic delay times and gravity anomaly data for regional structures: theory and synthetic examples. In *Upper mantle heterogeneities from active and passive seismology*, Proceedings of the NATO Advanced Research Workshop, Moscow, Russia, 155–168. [3] Nakamura, Y. (1983) Seismic velocity structure of the lunar mantle. *Journal of Geophysical Research* 88, 677–686. [4] Lognonné, P.; Gagnepain-Beyneix, G.; Charet, H. (2003) A new seismic model of the Moon: implications for structure, thermal evolution and formation of the Moon. *Earth and Planetary Science Letters*, 211, 27–44. [5] Khan, A.; Connolly, J. A. D.; MacLennan, J.; Mosegaard, K. (2007) Joint inversion of seismic and gravity data for lunar composition and thermal state. *Geophys. J. Int.* 168, 243–258. [6] Garcia, R.; Gagnepain-Beyneix, J.; Chevrot, S.; Lognonné, P. (2011) Very preliminary reference Moon model, *Physics of the Earth and Planetary Interiors* 198, 96–113.